



**Fermi National Accelerator Laboratory**

**FERMILAB-Conf-95/238-E**

**D0**

## **Inclusive $b$ Quark and Heavy Quarkonium Production at D0**

Kamel A. Bazizi

For the D0 Collaboration

*Fermi National Accelerator Laboratory  
P.O. Box 500, Batavia, Illinois 60510*

July 1995

To Appear in the Proceedings of the *10th Topical Workshop on Proton-Antiproton Collider Physics*,  
Fermilab, Batavia, Illinois, May 9-13, 1995

## Disclaimer

*This report was prepared as an account of work sponsored by an agency of the United States Government. Neither the United States Government nor any agency thereof, nor any of their employees, makes any warranty, expressed or implied, or assumes any legal liability or responsibility for the accuracy, completeness, or usefulness of any information, apparatus, product, or process disclosed, or represents that its use would not infringe privately owned rights. Reference herein to any specific commercial product, process, or service by trade name, trademark, manufacturer, or otherwise, does not necessarily constitute or imply its endorsement, recommendation, or favoring by the United States Government or any agency thereof. The views and opinions of authors expressed herein do not necessarily state or reflect those of the United States Government or any agency thereof.*

# Inclusive $b$ Quark and Heavy Quarkonium Production at $D\bar{O}$ \*

Kamel A. Bazizi  
For the  $D\bar{O}$  Collaboration

*Dept. of Physics and Astronomy  
University of Rochester  
Rochester, NY 14627  
USA*

## Abstract

We report the latest results on the measurement of inclusive  $b$  quark and heavy quarkonium production by the  $D\bar{O}$  collaboration in  $p\bar{p}$  collisions at  $\sqrt{s} = 1.8$  TeV at the Fermilab Tevatron Collider. The results are from analyses of the 1992-93 data. This report includes measurements of inclusive  $b$  quark,  $J/\psi$  and  $\Upsilon$  meson production cross sections. The  $b$  quark production cross section, measured in inclusive muon data, is consistent with next to leading order QCD predictions within theoretical and experimental errors. We study  $J/\psi$  and  $\Upsilon$  meson production in dimuon events and perform an investigation of the  $J/\psi$  production mechanisms. Including the latest developments in charmonium phenomenology, the  $J/\psi$  production rates are now almost all accounted for in the transverse momentum range above 8 GeV/c. The observed  $\Upsilon$  production rates, however, are higher than expected by a factor five.

---

\*To appear in the Proceedings of the Xth Topical Workshop on Proton-Antiproton Collider Physics, Fermilab, IL, May 9-13, 1995.

## INTRODUCTION

The study of  $b$  quark production in high energy hadronic interactions plays a crucial role in the testing of perturbative quantum chromodynamics (QCD) description of heavy quark production [1–3]. The study of heavy quarkonium production also plays an important role in testing QCD. Theoretical models of heavy quarkonium production are of particular importance because they involve both perturbative and non-perturbative QCD [4–6]. The basic ingredients of these calculations can be checked by comparing theoretical predictions with data.

We will briefly review the aspects of the DØ detector relevant to the analyses presented here. We present the results of a completed analysis of inclusive muon and  $b$  quark cross sections. We will also describe the analyses of inclusive  $J/\psi$  and  $\Upsilon$  production in dimuon data. Measurements of the inclusive  $J/\psi$  and  $\Upsilon$  production cross sections and a discussion of the  $J/\psi$  production mechanisms will be presented. We will close this report with a brief discussion of the analyses in progress and the future prospects for  $B$  physics at DØ.

## DØ DETECTOR

DØ is a large multi-purpose detector operating at the Tevatron  $p\bar{p}$  Collider, located at Fermi National Accelerator Laboratory. It features a non-magnetic inner tracking system, a compact and hermetic calorimeter and an extensive muon system. The DØ detector has been described in detail elsewhere [7] and only the features relevant for the analyses described here will be discussed briefly.

The inner tracking system covers a cylindrical region of radius 75 cm with wire drift chambers for the detection of charged tracks. The relatively small radius translates to a short decay path which makes muon contamination from in-flight decays of  $\pi/K$  minimal. The innermost tracking detector is a vertex drift chamber with a spatial resolution in the transverse plane of 60  $\mu\text{m}$ , and the outermost is a central drift chamber with a resolution of 180  $\mu\text{m}$ . Tracks in the central chamber are used to determine the primary interaction vertices, and together with the vertex chamber, enable the reconstruction of the muon impact parameter relative to the event primary vertex for  $b$  quark tagging.

The calorimeter is a uranium–liquid argon sampling detector, with a fractional electromagnetic energy resolution of  $15\%/\sqrt{E}$ , where  $E$  is in GeV, and a measured resolution for jets of  $75\%/\sqrt{E}$ .

The muon system covers the pseudorapidity range  $|\eta| < 3.3$ , and consists of three layers of chambers, with magnetized iron toroids located between the first and second layers. The magnetic field in the iron toroids is 1.9 T and provides a momentum measurement with a resolution,  $\sigma(1/p)/(1/p) = 0.18(p - 2)/p \oplus 0.008p$ , with  $p$  in GeV/c. The thickness of the calorimeter plus iron toroids varies from 14  $\lambda$  in the central region to 19  $\lambda$  in the forward region. This reduces the hadronic punchthrough background to a negligible level ( $< 0.5\%$ ) and allows a good identification of muons in jets.

## $\mu$ AND $b$ CROSS SECTIONS

Tagging  $b$  quarks through their semi-leptonic decays into muons has been standard in the study of  $b$  production. For moderately high  $p_T$ , muons come primarily from  $b$  quark decays. The standard technique for extracting a  $b$  cross section from inclusive muon data is to measure the muon cross section, determine the fraction of events coming from  $b$  decays, associate muon  $p_T$  with  $b$  quark  $p_T$ , and then correct for acceptance, branching ratio and fragmentation effects. The following is the analysis of inclusive muon data.

This analysis was based on data corresponding to a total integrated luminosity of  $\int \mathcal{L} dt = 75.6 \pm 4.1 \text{ nb}^{-1}$ . The data sample was obtained by filtering the interactions through a multi-level trigger. At the level 1 hardware trigger at least one muon candidate was required and the level 2 software trigger required at least one reconstructed muon track with transverse momentum  $p_T^\mu > 3 \text{ GeV}/c$ . Events were fully reconstructed off-line and retained for further analysis if they contained at least one muon track with rapidity  $|y^\mu| < 0.8$  and  $p_T^\mu > 3.5 \text{ GeV}/c$ . Candidate muons had to deposit  $> 1 \text{ GeV}$  of energy in the calorimeter; the mean energy loss for a single muon is about  $2.5 \text{ GeV}$ . A match was required with a good track in the central tracking detector pointing back to the primary interaction vertex. To minimize cosmic ray background, the reconstructed time of passage ( $t_0$ ) through the muon chambers had to be within  $100 \text{ ns}$  of the beam crossing. A total of  $15995$  muons passed all selections. Using ISAJET [8] Monte Carlo and data the total detection efficiency was estimated to be  $0.28 \pm 0.03$  for  $p_T^\mu \geq 6 \text{ GeV}/c$ . This analysis has been recently completed and published in Physical Review Letters [9]<sup>1</sup>.

### $b$ Fraction in Inclusive $\mu$ Events

Possible sources of backgrounds to muons from heavy flavor decays consist of cosmic rays, muons from Drell-Yan and  $J/\psi$  decays, and from  $\pi/K$  and  $W/Z$  decays. The residual cosmic ray contamination was estimated from the observed  $t_0$  distribution to be  $(9 \pm 3)\%$  and was subtracted from the data. Muons from Drell-Yan and  $J/\psi$  decays were estimated to contribute less than  $2\%$  of the data.

In obtaining the  $b$  quark cross section we restricted our analysis to muons in the  $p_T^\mu$  range  $4\text{--}30 \text{ GeV}/c$ . We estimated and subtracted the expected  $W/Z$  background. The remainder is expected to come mainly from  $b$  and  $c$  quark decays. To determine the fraction of muons from  $b$  quark decays,  $f_b$ , we used the transverse momentum of the muon with respect to the associated jet axis ( $p_T^{rel}$ ). Jets are reconstructed for  $E_T^{jet} > 8 \text{ GeV}$ , using a cone algorithm with radius  $R=0.7$ , where  $R = \sqrt{(\Delta\eta)^2 + (\Delta\phi)^2}$ . The  $p_T^{rel}$  distributions for  $b$  quark,  $c$  quark, and  $\pi/K$  decays were modeled with ISAJET.

Another interesting quantity in the study of heavy flavor production is the  $b$  fraction out of  $b$  and  $c$  decays,  $Q_b = N_b/(N_b + N_c)$ , which can be obtained by subtracting the  $\pi/K$

---

<sup>1</sup>In computing the cross sections of Ref. [9] we used  $\int \mathcal{L} dt = 73.3 \pm 8.8 \text{ nb}^{-1}$  instead of the more accurate luminosity measurement used in this report [12]. Therefore, the improved cross sections presented in this report are lower by  $\sim 3\%$  and their uncertainties are reduced by  $\sim 10\%$ .

contribution [9]. The relation between  $Q_b$  and  $f_b$  is simply  $Q_b = f_b/(1 - f_{\pi/K})$ , and at large  $p_T$  the  $\pi/K$  contribution is negligible and  $Q_b \simeq f_b$ . The measured  $Q_b$  distribution, compared to the result of ISAJET Monte Carlo simulation, is displayed in Fig. 1. The two results are consistent within errors but are slightly different in shape.

### $\mu$ Cross Section

The muon cross section due to inclusive  $b$  quark decays can be obtained by correcting for the total efficiency, the fraction due to  $b$  decays and the muon momentum resolution using the technique of Reference [13]. The results, including the statistical and systematic errors are summarized in Table I. The spectrum shown in Fig. 2 is extracted without assumptions concerning heavy flavor production cross sections, and represents our experimental result. The theoretical spectrum was calculated using ISAJET for  $b$ -quark production, fragmentation and decay, with the cross section normalized to the NLO QCD calculation [1]. We used the Peterson fragmentation function with  $\epsilon_b = 0.006 \pm 0.003$  [14] and the average LEP inclusive branching ratio  $\text{Br}(B \rightarrow \mu) = 0.110 \pm 0.005$  [15].

### $b$ Quark Production Cross Section

We extracted the  $b$  quark production cross section from the muon spectrum following the method described in References [9–11]. The resulting cross section as a function of  $p_T^{min}$ , for  $|y^b| < 1.0$ , is shown in Fig. 3.  $p_T^{min}$  refers to the  $b$  quark  $p_T$  above which 90% of the muons originate from  $b$  quarks with  $p_T > p_T^{min}$ . The results including the statistical and systematic errors are summarized in Table II. The curves represent the NLO QCD predictions [1] using MRSDØ parton distribution functions [17]. The QCD mass scale  $\Lambda_{\overline{MS}}^{(5)} = 140$  MeV and the renormalization and factorization scale  $\mu = \mu_0$  (with  $\mu_0^2 = m_b^2 + (p_T^b)^2$ , and  $m_b = 4.75$  GeV/ $c^2$ ) were used for the solid curve, and customary variations of these parameters for the dashed curves: 187 MeV and  $\mu_0/2$  (upper), and 100 MeV and  $2\mu_0$  (lower).

This result is in close agreement with our  $b$  cross section measurement in inclusive dimuon data [18]. Another analysis is in progress to determine the  $b$  production cross section from the study of the properties of muons plus jets. We also expect to obtain other  $b$  cross section measurements through the study of the spatial  $b\bar{b}$  correlations, where the measurement of the opening angle between muon pairs in the transverse plane allows the separation of the LO and NLO contributions.

### INCLUSIVE $J/\psi$ PRODUCTION

Previous calculations of  $J/\psi$  production in  $p\bar{p}$  collisions have assumed that the dominant contribution to the cross section comes from leading order diagrams with  $gg$  fusion into a charmonium state and a recoiling gluon [4], and  $b\bar{b}$  pair production followed by  $b \rightarrow J/\psi + X$  decay [3,5]. These calculations, however, did not explain all the observed rates at hadron colliders [19,20], which suggested that there were other possible important production mechanisms. This has inspired theorists to investigate higher order processes. It has been

suggested recently that the dominant mechanism for charmonium production at large  $p_T$  is fragmentation [21], which is the production of a high  $p_T$  gluon or charm quark which subsequently fragments into charmonium states ( $J/\psi$ ,  $\chi_c$ ).

### Inclusive $J/\psi$ Cross Section

We have studied  $J/\psi$  production at DØ using opposite sign dimuon events. The analysis where we measured the inclusive cross section was based on a total integrated luminosity of  $\int \mathcal{L} dt \approx 6.6 pb^{-1}$ , while the analysis where the fraction of  $J/\psi$  events coming from  $b$  decays and the fraction produced through  $\chi_c$  radiative decays were investigated, was based on a larger sample  $\approx 13 pb^{-1}$ . Events were collected by requiring at least two muon candidates at the level 1 trigger. At level 2, at least two muon tracks had to be reconstructed and pass some loose track quality cuts with a minimum  $p_T$  of 3 GeV/c on each muon. The offline selection of each muon track was similar to that of the inclusive muon sample. In addition, the muon pairs were restricted to be within the kinematic range  $|\eta^{\mu\mu}| < 0.6$  and  $p_T^{\mu\mu} > 8$  GeV/c. In this analysis we investigated the dimuon mass range  $0.2 < M^{\mu\mu} < 6$  GeV/c<sup>2</sup>. A total number of 1221 events passed all selection criteria with an overall efficiency of  $2.8 \pm 0.3\%$ .

The invariant mass,  $M^{\mu\mu}$ , distribution for the opposite sign muon pairs is shown in Fig. 4. We observed a  $J/\psi$  signal with a mass resolution well represented by a Gaussian function. The dominant contribution to  $J/\psi$  background is expected to come from  $b\bar{b}$ ,  $c\bar{c}$  and  $\pi/K$  decays. Other mechanisms that yield dimuons in the  $J/\psi$  mass region are Drell-Yan processes and decays of the light quark mesons  $\rho$ ,  $\phi$  and  $\eta$ .

The invariant mass width is dominated by the muon momentum resolution where  $\Delta M^{\mu\mu}/M^{\mu\mu} = (1/\sqrt{2})(\Delta p^\mu/p^\mu)$ .  $\Delta M^{\mu\mu}$  is expected to be 0.4 GeV/c<sup>2</sup> at the  $J/\psi(1S)$  mass of 3.1 GeV/c<sup>2</sup>, and 0.5 GeV/c<sup>2</sup> at the  $\psi(2S)$  mass of 3.7 GeV/c<sup>2</sup>. Because the difference between the masses of the two states is of the same order of magnitude as the mass resolution, it is difficult to distinguish the two states. On the other hand, due to the suppression of the decay  $\psi(2S) \rightarrow \mu^+\mu^-$  (0.77%) compared to  $J/\psi(1S) \rightarrow \mu^+\mu^-$  (5.97%) [22], the expected contribution to the  $J/\psi(1S)$  sample from  $\psi(2S)$  should be small.

Muons originating from  $b$  and  $c$  decays are usually accompanied by a jet of hadrons. Gluon and charm fragmentation into charmonium is also expected to produce muons inside jets. By contrast, muons from Drell-Yan events and those coming from the direct charmonium production are expected to be isolated. In order to distinguish these processes we selected the variables  $M^{\mu\mu}$ ,  $p_T^{rel\mu\mu}$  and  $I^{\mu\mu}$ . We define the isolation parameter for a muon,  $I^\mu$ , as the difference between the observed energy in the calorimeter, within a cone of radius  $R = 0.3$  around the muon direction, and the expected energy deposition for a minimum ionizing particle, weighted by the energy measurement uncertainty. The isolation parameter for a muon pair,  $I^{\mu\mu}$ , is the isolation of the more energetic muon.

For each process we parametrized the distributions for the selected variables using a full Monte Carlo simulation consisting of ISAJET, detector [23] and trigger simulations. We then applied the maximum likelihood method to determine the relative contribution of each process. The resulting mass distributions for all the contributions are shown in Fig. 4. From the fit, the total number of dimuon events due to  $J/\psi \rightarrow \mu^+\mu^-$  is  $407 \pm 28$ .

The  $J/\psi$   $p_T$  distribution resulting from the fit was then unfolded [13] and corrected for acceptance and efficiency. The differential  $J/\psi$  production cross section as a function of the  $J/\psi$   $p_T$  is shown in Fig. 5. The data points are shown with the statistical and systematic errors added in quadrature. The total systematic uncertainty of  $\sim 22\%$  includes contributions from trigger efficiency (15%), background subtraction (14%), offline dimuon selection cuts (5%) and the integrated luminosity (5%). After accounting for the contribution due to fragmentation, the theoretical predictions describe our spectrum reasonably well. It should also be noted that our spectrum agrees closely in normalization and shape with the  $J/\psi$  inclusive cross section measured by the CDF collaboration [20]. By integrating over all bins we obtain a total cross section of:

$$Br(J/\psi \rightarrow \mu^+ \mu^-) \cdot \sigma(p\bar{p} \rightarrow J/\psi + X) = 1.93 \pm 0.16(\text{stat}) \pm 0.43(\text{syst}) \text{ nb},$$

$$p_T^{J/\psi} > 8.0 \text{ GeV}/c \quad \text{and} \quad |\eta^{J/\psi}| < 0.6$$

### **$b$ Decay Channel: $b \rightarrow J/\psi + X$**

$b$  quarks may be tagged through  $J/\psi$  production, since a good fraction of  $J/\psi$  events is expected to come from  $b$  decays. To determine this fraction we have examined the distribution of the impact parameter of the muons relative to the event vertex, in the transverse plane to the beam axis. Each muon was required to have a matching track in the central drift chamber and in the vertex drift chamber. We have performed a simultaneous mass and impact parameter maximum likelihood fit to the opposite sign dimuon data in the mass range 2 - 4.4  $\text{GeV}/c^2$  and the impact parameter range  $-0.08$  cm to 0.16 cm. The muon impact parameter distribution together with the results of the fit is shown in Fig. 6. More details on this analysis can be found in Reference [24].

### **Radiative Decay Channel: $\chi_c \rightarrow J/\psi + \gamma$**

One of the  $J/\psi$  production mechanisms is through the radiative decay of  $\chi_{c0}$ ,  $\chi_{c1}$ ,  $\chi_{c2}$  states. The masses of the  $\chi_{c0,1,2}$  states are 3.42, 3.51, 3.56  $\text{GeV}/c^2$  respectively [22]. The width of the experimental distribution  $\Delta M$ , which is a characteristic of the photon energy and is defined below, is dominated by the photon energy resolution,  $15\%/\sqrt{E}$ . For a photon energy of 1 GeV the expected width of  $\Delta M$  is 0.06  $\text{GeV}/c^2$  at the peak of 0.4  $\text{GeV}/c^2$ . This resolution is not sufficient to observe the different  $\chi_c$  states separately and the result will therefore pertain to the inclusive  $\chi_c$  production.

We investigated the production of  $J/\psi$  through the  $\chi_c$  radiative decay by fully reconstructing the decay chain  $\chi_c \rightarrow J/\psi + \gamma, J/\psi \rightarrow \mu^+ \mu^-$ . The data sample consisted of opposite sign muon pairs in the  $J/\psi$  mass range, defined as  $2 < M^{\mu\mu} < 4 \text{ GeV}/c^2$ . We then searched for photons with energy greater than 1 GeV, in the cone  $R = 2$  about the muon pair with an efficiency of  $\epsilon_\gamma = 30 \pm 4\%$ . We found a total number of  $N_{J/\psi} = 722$  events above background. The invariant mass difference between the  $\mu\mu\gamma$  and  $\mu\mu$  systems,  $\Delta M$ , where a clear  $\chi_c$  signal is observed, is shown in Fig. 7.

To obtain the number of  $\chi_c$  signal events we performed a fit of the  $\Delta M$  distribution to a Gaussian signal plus background. The background shape was obtained from data by combining dimuons with electromagnetic clusters from different events. The fit resulted in  $N_\chi = 66 \pm 15(\text{stat}) \pm 5(\text{syst})\chi_c$  events. The measured fraction of  $J/\psi$  events coming from  $\chi_c$  decay is obtained as  $f_\chi = N_\chi/(N_{J/\psi} \cdot \epsilon_\gamma) = 0.30 \pm 0.07(\text{stat}) \pm 0.07(\text{syst})$ . Our result is similar to that obtained by the CDF collaboration [25] using a similar technique.

## INCLUSIVE $\Upsilon$ PRODUCTION

The study of  $\Upsilon$  production in  $p\bar{p}$  collisions is particularly interesting because it allows us to test the existing bottomonium production models by investigating the different production mechanisms. The various  $\Upsilon$  states are expected to be produced through direct  $gg$  fusion or indirect production through radiative decay of  $\chi_b$  states. Unlike the  $J/\psi$  cross section, which is limited to  $p_T > 8$  GeV/c by the detector acceptance, the  $\Upsilon$  cross section can be extended down to  $p_T = 0$ . This allows the study of the low  $p_T$  region where fragmentation is not expected to dominate.

The masses of the states  $\Upsilon(1S, 2S, 3S)$  are 9.5, 10.0, 10.4 GeV/c<sup>2</sup>, respectively [22]. On the other hand the expected mass resolution at the  $\Upsilon(1S)$  mass, which is dominated by the muon momentum resolution, is 1.3 GeV/c<sup>2</sup>. Therefore we do not expect to resolve the three different states but perform an inclusive observation of all states combined.

### Dimuon Mass Distribution

The  $\Upsilon$  study at DØ was based on a data sample of opposite sign dimuons corresponding to a total integrated luminosity of  $\int \mathcal{L} dt = 6.6 \pm 0.4$  pb<sup>-1</sup>. The data were collected using a multilevel trigger with similar conditions as the  $J/\psi$  data. In addition to selecting each muon in a similar fashion to the inclusive muon data, both muons were required to be isolated such that  $I^\mu < 3$ . To minimize the contamination from high  $p_T$  cosmic ray muons penetrating completely through the detector and appearing as dimuons, the opening angle between the two muons was restricted to be less than 165°. In addition, the muon pairs were restricted to be within the kinematic range  $|\eta^{\mu\mu}| < 0.7$  and  $0 < p_T^{\mu\mu} < 25$  GeV/c. In this analysis we investigated the dimuon mass range  $6 < M^{\mu\mu} < 35$  GeV/c<sup>2</sup>. A total number of 240 events passed all selection criteria with an overall efficiency of  $1.2 \pm 0.2\%$ .

Contributions to dimuon events in the  $\Upsilon$  mass region are expected to come from QCD processes ( $b\bar{b}$ ,  $c\bar{c}$  and  $\pi/K$ ), Drell-Yan decays and cosmic rays. In order to distinguish these processes we used the variables  $M^{\mu\mu}$ ,  $H$  and  $t_0$ , where  $t_0$  is the timing offset relative to beam crossing and  $H$  is the isolation parameter defined as the energy difference between two concentric cones of radii  $R = 0.6$  and  $0.2$  around the muon direction. We used data to obtain the  $H$  distribution for both  $\Upsilon$  signal and QCD processes. The  $\Upsilon$ , QCD and Drell-Yan mass shapes were taken from a fully simulated Monte Carlo, while the shape for the cosmic contribution was taken from cosmic ray data which was also used to determine the  $t_0$  cosmic ray distribution. A different data sample with tight cuts was used to extract the  $t_0$  shape corresponding to beam related dimuon events. The signal and background contributions were then determined by performing a simultaneous maximum likelihood fit of the selected

distributions to the data. The number of  $\Upsilon$  signal events resulting from the fit is  $85 \pm 11$ , which is about 35% of the total event sample. The dimuon mass distribution along with all the different contributions is shown in Fig. 8.

### Inclusive $\Upsilon$ Cross Section

The  $\Upsilon$   $p_T$  distribution resulting from the fit was then unfolded [13] and corrected for acceptance and efficiency. The obtained differential cross section as a function of the  $\Upsilon$   $p_T$  is displayed in Fig. 9. Also shown is a solid curve representing the theoretical predictions for  $\Upsilon$  production [4,6] with MRSD $\emptyset$  parton distribution functions. The predictions include the production of  $\Upsilon(1S)$ ,  $\Upsilon(2S)$  and  $\Upsilon(3S)$  states directly and through radiative decays of higher  $\chi_b$  states. The data points are higher than the theoretical predictions by a factor five except at low  $p_T$ . The shape of our distribution differs from the theory at low  $p_T$ . The inner error bars are statistical and outer systematic. The total systematic uncertainty includes contributions from trigger efficiency, momentum resolution correction, sign determination and the opening angle cut. There is an additional 15% overall uncertainty to the normalization not included in the figure; it includes uncertainties in the distributions used in the fit (12%), selection cuts (7%) and luminosity (5%). By integrating over all bins we obtain a total cross section of:

$$Br(\Upsilon \rightarrow \mu^+ \mu^-) \cdot \sigma(p\bar{p} \rightarrow \Upsilon + X) = 1.12 \pm 0.12(\text{stat}) \pm 0.22(\text{syst}) \text{ nb},$$

$$p_T^\Upsilon > 0 \text{ GeV}/c \quad \text{and} \quad |y^\Upsilon| < 0.7$$

The existing calculations for heavy bottomonium production have provided a reasonable description of the lower energy data. These predictions are clearly inadequate to explain our measured  $\Upsilon$  rates at the Tevatron energy. The fact that fragmentation processes are not expected to contribute considerably in the low  $p_T$  region suggests that other states and production mechanisms may exist [26]. It should be noted that our measurement is in reasonable agreement with that of the CDF collaboration [27].

### B PHYSICS FUTURE PROSPECTS AT D $\emptyset$

The results presented here are obtained from analyses of the 1992-93 data. These analyses are restricted to the central region of the D $\emptyset$  detector. We have begun to explore the forward region, which is of particular importance because it is the region where the cross sections are most sensitive to the gluon distribution. By analyzing a dimuon data sample based on a total integrated luminosity of  $4.6 \text{ pb}^{-1}$  from the 1994-95 run we have observed a  $J/\psi$  signal in the region  $2.6 < |\eta^{J/\psi}| < 3.4$ . The corresponding opposite sign dimuon mass distribution is shown in Fig. 10. A fit to a Gaussian signal and exponential background, in the mass range  $2.1 < M^{\mu\mu} < 4.5 \text{ GeV}/c^2$ , yields a total number of 198 signal events above a background of 36.

To pin down the fraction of  $J/\psi$  events coming from  $b$  decays, in addition to the impact parameter technique, an analysis of trimuon events, where one  $b$  is tagged with a  $J/\psi$  and the other with a muon, is in progress. A perturbative QCD test is also being performed

through the measurement of heavy flavor content in inclusive jets, which further allows the study of parton fragmentation for gluons,  $b$  and  $c$  quarks.

## CONCLUSIONS

The  $D\bar{O}$  experiment has demonstrated the ability to study  $b$  production in hadronic collisions with reasonable efficiency and background rejection. Our  $b$  production cross section measurements indicate that NLO QCD calculations describe heavy flavor production within the experimental and theoretical errors. Although there is a residual discrepancy of  $\sim 50\%$  in magnitude between the central values, the  $p_T$  shapes are in good agreement over the entire  $p_T$  range. A precise agreement of the theory and data can be obtained with extreme values for  $\Lambda_{QCD}$  and the scale  $\mu$ . We have observed the charmonium states  $J/\psi$  and inclusive  $\chi_c$ . We have measured the inclusive  $J/\psi$  cross section and it is almost all accounted for in the  $p_T$  range above 8 GeV/ $c$ , when including the fragmentation production mechanisms. We have also observed an inclusive  $\Upsilon$  signal and measured the corresponding production cross section down to  $p_T = 0$ . Our preliminary measured rate is higher than existing theoretical predictions by a factor five. Our data suggest that other states and production mechanisms at the Tevatron energy may be important. Several analyses are in progress and five times more data should provide us with a better understanding of  $b$  production properties in  $p\bar{p}$  collisions.

## ACKNOWLEDGEMENTS

We appreciate the substantial contributions to this work on the part of the Fermilab Accelerator, Computing and Research Division staffs. We would like to thank Michelangelo Mangano for providing us with his heavy quarkonium code.

## REFERENCES

- [1] P. Nason, S. Dawson and R.K. Ellis, Nucl. Phys. **B327**, 49 (1989).
- [2] W. Beenakker, W.L. van Neerven, R. Meng, G.A. Schuler and J. Smith, Nucl. Phys. **B351**, 507 (1991).
- [3] M. Mangano, P. Nason and G. Ridolfi, Nucl. Phys. **B373**, 295 (1992).
- [4] R. Baier and R. Ruckl, Z. Phys. **C19**, 251 (1983).
- [5] E. W. N. Glover, A. D. Martin and W. J. Stirling, Z. Phys. **C38**, 473 (1988).
- [6] M. L. Mangano, "Quarkonium Production Codes", (unpublished).
- [7] DØ Collaboration, S. Abachi *et al.*, Nucl. Instr. Meth. **A338**, 185 (1994).
- [8] F. Paige and S. Protopopescu, BNL Report no. BNL-38034, 1986 (unpublished), release v 7.0.
- [9] DØ Collaboration, S. Abachi *et al.*, Phys. Rev. Lett. **74**, 3548 (1995).
- [10] CDF Collaboration, F. Abe *et al.*, Phys. Rev. Lett. **71**, 500, 2396, 2537 (1993).
- [11] UA1 Collaboration, C. Albajar *et al.*, Phys. Lett. **B256**, 121 (1991).
- [12] J. Bantly *et al.*, Internal DØ Note **2544**, Apr. 26, 1995, Fermilab-TM-1930.
- [13] G. D'Agostini, DESY 94-099, June 1994.
- [14] C. Peterson *et al.*, Phys. Rev. D **27**, 105 (1983); J. Chrin, Z. Phys. C **36**, 163 (1987).
- [15] S. Squarcia, "Heavy Flavor Physics at LEP," CERN-PPE/94-69 (1994).
- [16] G. D. Lafferty and R. Wyatt MAN/HEP/94/3, CERN-PPE/94-72, (May 6 1994).
- [17] A. Martin, R. Roberts, J.W. Stirling, Phys. Rev. D **47**, 867 (1993).
- [18] S. Febers for the DØ Collaboration, these proceedings.
- [19] UA1 Collaboration, C. Albajar *et al.*, Phys. Lett. **B256**, 112, (1991).
- [20] CDF Collaboration, F. Abe *et al.*, Phys. Rev. Lett. **69**, 3704 (1992).
- [21] E. Braaten *et al.*, FERMILAB-PUB-94/135-T.
- [22] Particle Data Group, L. Montanet *et al.*, "Review of Particle Properties," Phys. Rev. D **50**, 1173 (1994).
- [23] F. Carminati *et al.*, "GEANT Users Guide," vs. 3.15, CERN Program Library, December 1991 (unpublished).
- [24] C. Murphy, Ph.D. thesis, Indiana University, Bloomington, (1995) (unpublished).
- [25] CDF Collaboration, F. Abe *et al.*, Phys. Rev. Lett. **71**, 2537 (1993).
- [26] M. L. Mangano, these proceedings.
- [27] V. Papadimitriou for the CDF Collaboration, FERMILAB-Conf-94/221-E.

## TABLES

TABLE I. A summary of the unfolded  $b$  produced muon cross section, the statistical and systematic uncertainties as a function of the muon transverse momentum  $p_T^\mu$ .  $p_T^\mu$  is computed using the algorithm of reference [16].

$p_T^\mu$ bin (GeV/c)	$p_T^\mu$ (GeV/c)	$\frac{d\sigma_b^\mu}{dp_T^\mu}$ [nb/(GeV/c)]	Statistical [nb/(GeV/c)]	Systematic [nb/(GeV/c)]
4-5	4.5	66.192	0.861	17.872
5-6	5.5	37.251	0.671	6.705
6-8	6.9	15.888	0.318	2.860
8-10	8.9	5.312	0.197	0.956
10-12	10.9	2.237	0.132	0.403
12-15	13.3	0.938	0.075	0.169
15-19	16.9	0.366	0.039	0.073
19-24	21.2	0.102	0.018	0.024
24-30	26.7	0.027	0.009	0.008

TABLE II. A summary of the inclusive  $b$  quark production cross section integrated above a certain  $p_T^{min}$ , the statistical and systematic uncertainties as a function of the  $b$  quark  $p_T$ .

$p_T^{min}$ (GeV/c)	$\sigma^b(p_T^b > p_T^{min})$ (nb)	Statistical (nb)	Systematic (nb)
6	6884.0	89.5	2202.9
7	5362.0	96.5	1340.5
9	2895.2	57.9	723.8
12	1167.1	43.2	291.8
15	566.9	33.5	141.7
19	258.0	20.6	64.5
23	152.3	16.3	41.1
30	51.4	9.1	14.9
38	18.9	6.2	6.2

## FIGURES

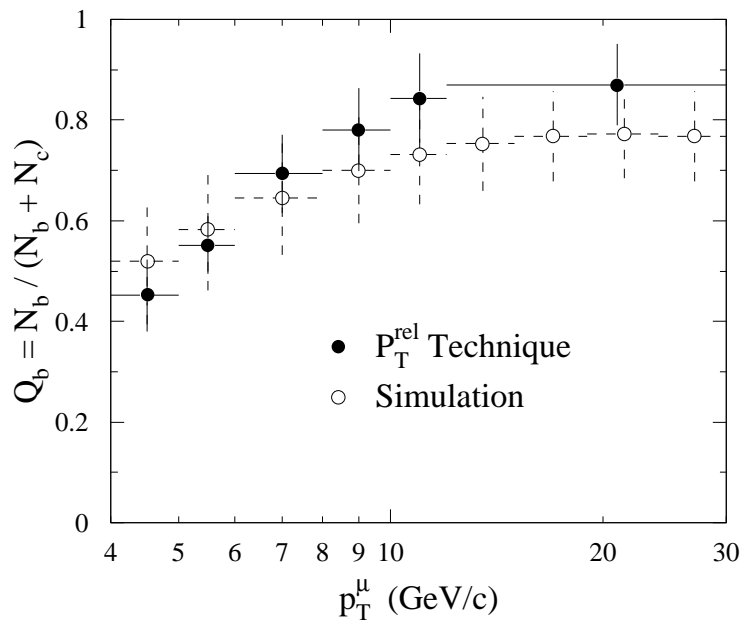


FIG. 1. The measured  $b$  fraction ( $Q_b$ ) using  $p_T^{rel}$  technique, compared to the result of a simulation using ISAJET Monte Carlo, as a function of the muon  $p_T$ .

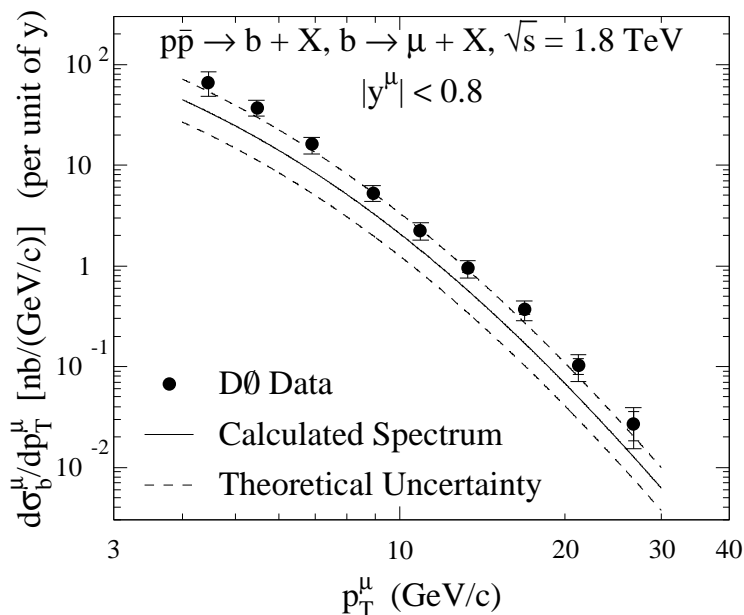


FIG. 2. The unfolded muon cross section corresponding to inclusive  $b$  decays compared to the expected spectrum (see text for details). Inner error bars are statistical and outer statistical and systematic added in quadrature.

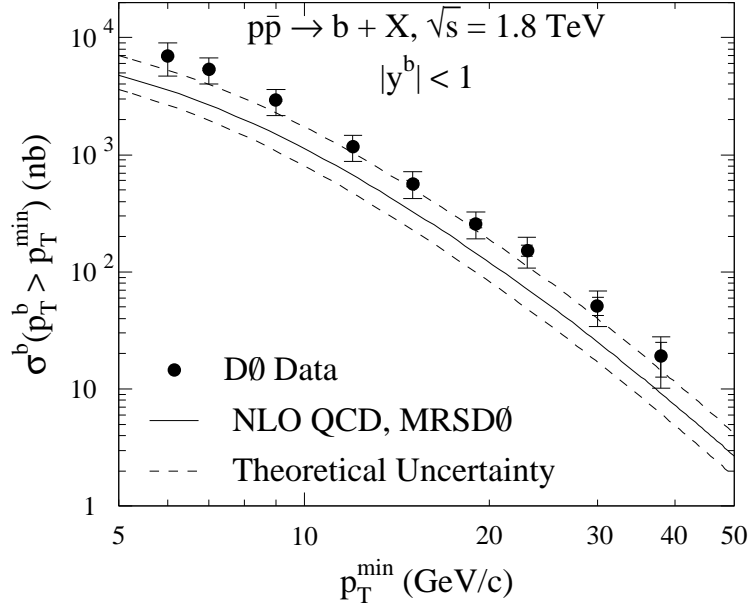


FIG. 3. The  $b$  quark production cross section compared to NLO QCD predictions (see text for details). Inner error bars are statistical and outer statistical and systematic added in quadrature.

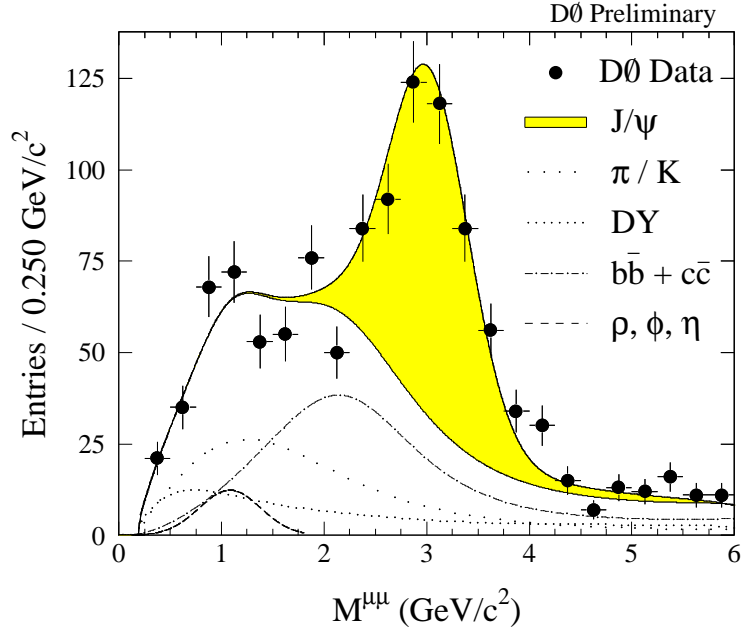


FIG. 4. The dimuon mass distribution in the range  $0.2 < M^{\mu\mu} < 6 \text{ GeV}/c^2$ . The hatched area indicates the  $J/\psi$  signal on the top of the sum of the background contributions, which are also shown separately.

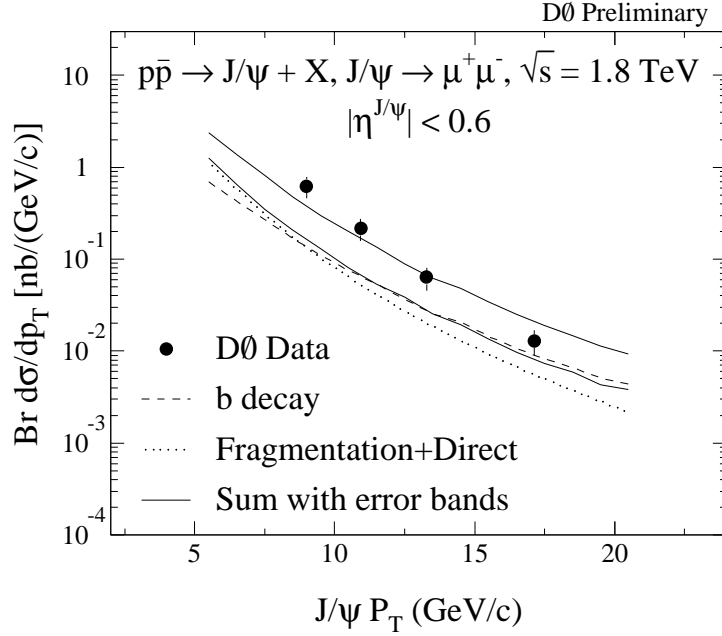


FIG. 5. The  $J/\psi$  production cross section  $Br \cdot d\sigma/dp_T$  as a function of the  $J/\psi$   $p_T$ . The error bars are statistical and systematic added in quadrature. The solid curves represent the error band on the sum of the expected contributions.

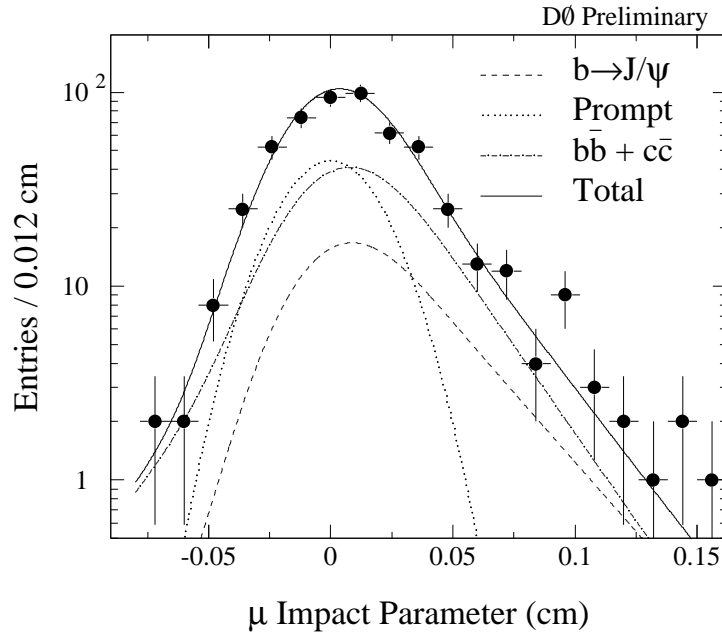


FIG. 6. The muon impact parameter distribution with respect to the event vertex in the transverse plane. Also shown are the fitted contributions from prompt and non-prompt  $J/\psi$  sources.

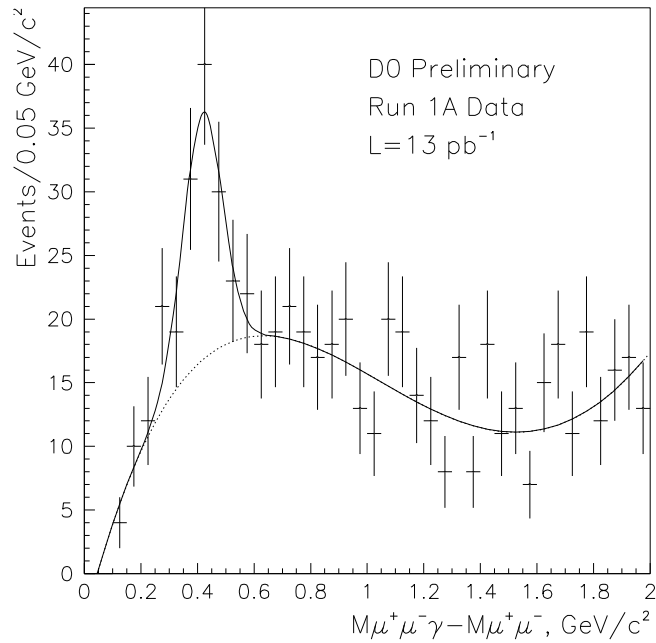


FIG. 7. The distribution of the mass difference  $\Delta M$  for dimuon events in the  $J/\psi$  mass region. The data are shown as points. The solid curve is a fit to a Gaussian plus the background shape (see text).

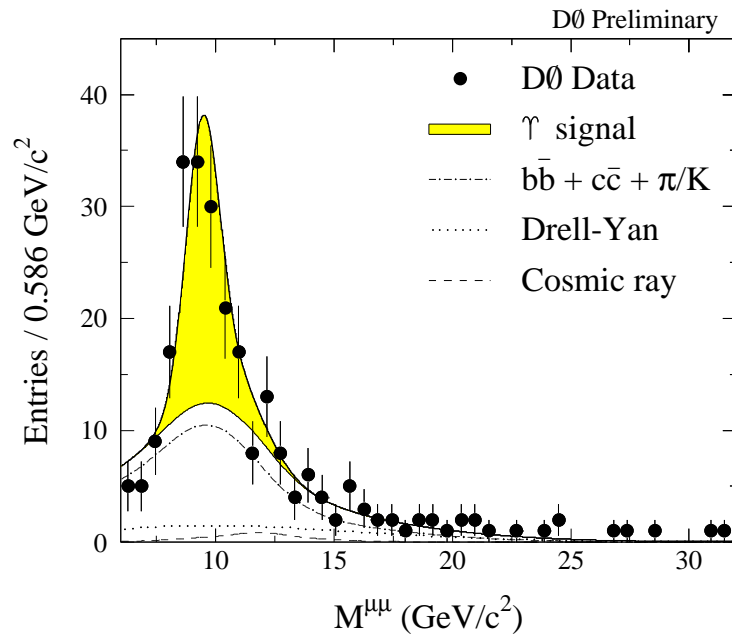


FIG. 8. The dimuon mass distribution in the range  $6 < M^{\mu\mu} < 35 \text{ GeV}/c^2$ . The hatched area indicates the  $\Upsilon$  signal on the top of the sum of the background contributions, which are also shown separately.

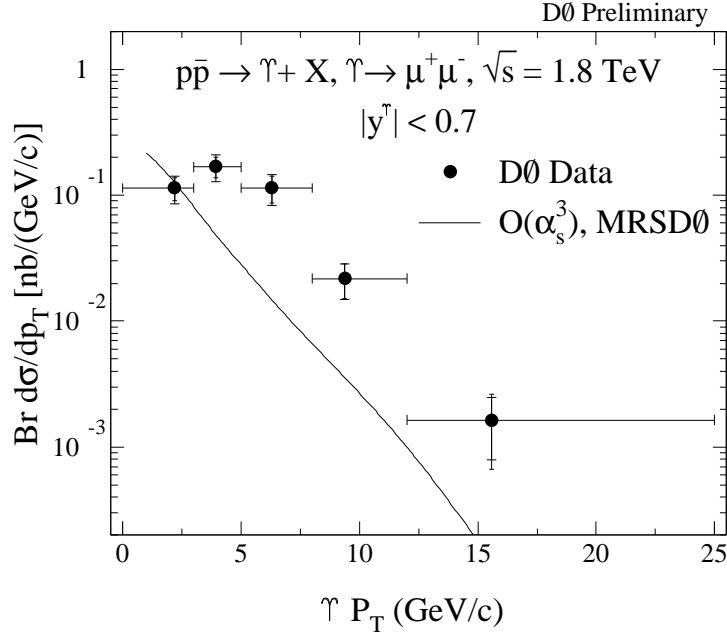


FIG. 9. The  $\Upsilon$  production cross section  $Br \cdot d\sigma/dp_T$  as a function of the  $\Upsilon$   $p_T$ . The error bars are statistical and systematic (wider ticks), shown separately. The curve represents the theoretical predictions for  $\Upsilon$  production (see text).

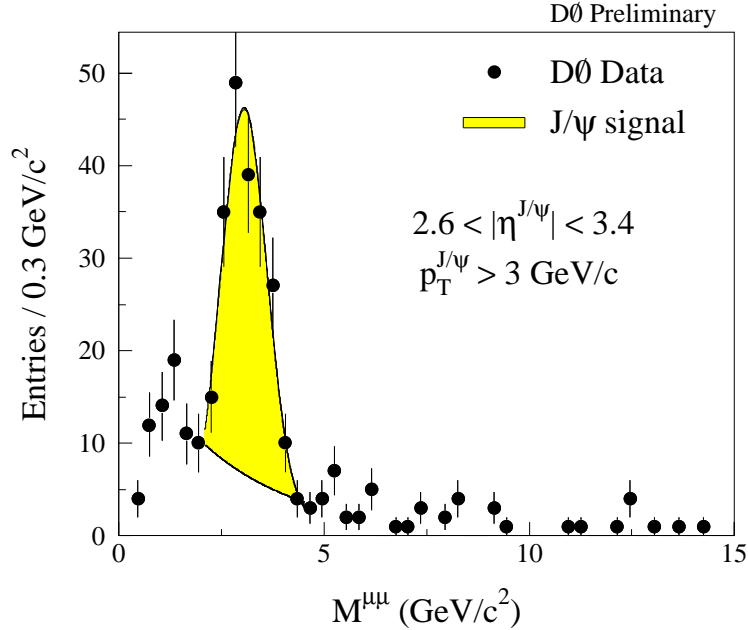


FIG. 10. The invariant mass distribution for opposite sign muon pairs in the D0 forward muon detector  $2.6 < |\eta^{\mu\mu}| < 3.4$ . The solid curve is the fitted sum of the  $J/\psi$  signal (hatched area) and background contribution in the mass range  $2.1 < M^{\mu\mu} < 4.5 \text{ GeV/c}^2$ .